Underwater Image Enhancement by Combining LAB Color Space and Double-Opponency Mechanism

Xing Huang, Yujuan Sun, Xiaofeng Zhang, Jiaxing Zhang*

School of Information and Electrical Engineering,
Ludong University,
China
2717971050@qq.com, sunyujuan@ldu.edu.cn, iamzxf@126.com, z924554650@163.com

Abstract

The captured underwater images often have color distortion and blur due to the propagation characteristics of light in water. The enhancement for underwater images using deep learning has shown promising prospect. However, most neural networks model the inputs and outputs end-to-end directly, which fails to fully utilize the inherent information present in underwater images. We focus more on the real color distribution in water that contains comprehensive information, and fully leverage these information to restore the underwater images without the color deviation. In this work, an underwater image enhancement model combining Lab color space and double-opponency mechanism is proposed. Lab color space can extract luminance and chroma, which can express wider chroma range based on human visual perception. Double-opponent mechanism can extract color constancy features based on the biological vision mechanism when the lights have attenuation differences. Moreover, an adaptive light estimation module is designed to learn the light map from the outputs of double-opponency to adjust the overall color of the images. Extensive experiments demonstrate that our approach achieves outstanding results in enhancing color and clarity in underwater images.

Keywords: Underwater image, Image enhancement, Color correction, Color space

1 Introduction

Underwater images are widely used in the marine biology, underwater robot exploration, and other fields. However, different wavelengths of light in water have different attenuation due to the absorption properties in water [1], and the captured underwater images will show serious color deviation. As the red light attenuates quickly in water, blue and green lights slowly, the captured images often appear the bluish or greenish tinge [2]. At the same time, the suspended particles in water will also produce a scattering blur in captured images [3]. These issues seriously affect the optical imaging quality of underwater images, and also reduce the accuracy of the image detection and segmentation. Therefore, underwater image enhancement [4-8] is regarded as a crucial foundation for underwater resource detection and exploration [9]. We aim to improve the quality and visibility of underwater images to make them more suitable for human visual perception [10].

Figure 1. The image shows a comparison between the enhanced version on the left and the distorted version on the right

The previous traditional methods mainly use the underwater imaging model proposed by JAFF [11] combined with the relevant prior assumptions to enhance the underwater images, such as DCP [12] and the red channel [13]. These methods are mainly used to predict the unknown parameters of the imaging model by inverse solution, and then adjust the color of the captured image. However, traditional model-based approaches [14-16] are limited by specific aquatic environments, and difficult to generalize their applicability across diverse underwater settings. The utilization of the deep learning approach presents a vast potential for enhancing underwater image quality, such as [17-21]. But most neural networks model the inputs and outputs end-to-end directly. There is still deviation of color brightness or saturation in underwater image recovery.

One of the important reasons may be that some latent information of underwater images is not completely used. So in this paper, we extract luminance and chroma information based on Lab space, which has a wider chroma range and contains richer information than RGB color space. Another reason is that current optical imaging devices do not have the ability of perceiving color constancy like the human vision system, which can

*Corresponding Author: Yujuan Sun; Email: sunyujuan@ldu.edu.cn
DOI: https://doi.org/10.70003/160792642025112606006

enable the object's perceived color constant when the light environment changes. Inspired by double-opponency mechanism of the human visual system [22], we extract color constancy features based on opponent color space when the lights have attenuation differences. The space has a special sensitivity to color contrast, that is, the values of different color channels will change when the light spectrum distribution changes, but their difference does not change obviously. This property can be used to extract the whole light source information for compensating the image color.

In this paper, we design a dual encoder-decoder enhancement model that fuses Lab and double-opponency to restore the degenerated underwater images. Moreover, an adaptive light estimation module is designed to learn the light map from the outputs of shallow feature extractor to control the whole color of the underwater images. We use both the synthetic dataset [23] and the real dataset UIEB [24] to train the proposed model. Figure 1 displays the enhanced result. The contributions of this paper are as follows:

- An underwater image enhancement model is proposed by combining Lab color space and double-opponency mechanism, which effectively fuses a wider chroma range information and the color constant property of the human visual system.
- An adaptive light estimation module is designed from the outputs of double-opponency module to compensate for the color bias caused by attenuation, which can control the overall image color.
- Considering the difficulty of obtaining underwater pairs of distorted images and clear counterparts, the synthetic and real datasets are employed to train the proposed model together, and these training data can not only reflect the diversity and complexity of different water types but also enhance authenticity and practicality in application.

Extensive comparative experiments have been conducted with previous underwater image enhancement methods to verify the superiority of the proposed method.

2 Related Work

2.1 Traditional Methods for Underwater Image Enhancement

There are two main types of methods for enhancing underwater images in the past: physics-based and non-physics-based methods. Non-physics-based methods attempted to achieve better clarity and color for underwater images by adjusting the pixel values, such as histogram equalization [25], gray world assumption [26], etc. These methods may suffer from unnatural colors or image distortion and have limited applicability. Physics-based methods relied on the underwater image degradation formula and predicted the parameters of the formula from the given image, then reconstructed a clear image by inverse inference, such as red channel prior [13], blurriness prior [17], etc. These methods mainly focused on estimating the transmission map of the images and then recovering the images using the degradation formula. However, the uncertainty of underwater scenes may prevent these methods from producing satisfactory results.

2.2 Underwater Image Enhancement Based on Deep Learning

Recently deep learning has made significant improvements in underwater image restoration, it can build a highly complex function from a large amount of data, which can effectively remove the degradation of underwater images. WaterGan [27] proposed a two-stage network that first generates synthetic underwater images using RGB-D and real underwater images, then used these synthetic images to train an image restoration network. Fabbri et al. [28] proposed UGAN which trained on the dataset synthesized by CycleGAN [18] and introduced a gradient difference loss to prevent the generated image from being too blurry. The GAN-based methods mentioned above have high training difficulty and often produce undesired image artifacts. WaterNet [24] was trained on a self-built the UIEB dataset and used the fusion of different confidence maps to improve clarity. Peng et al. [29] designed a loss function that combines multi-color spaces to remove color artifacts. Ucolor [30] combined the advantages of Lab and HSV color spaces to enhance images. Despite using multi-color spaces to enhance the color features, the water removal effect is unsatisfactory. UWCNN [23] proposed an enhanced network combining imaging model, which generates an approximate ground truth image. MetaUE [31] combined with the physical model used the meta-learning strategy to estimate the unknown parameters, which can solve the different degradation issues. However, considering the complexity of the real underwater scene, accurately estimating parameters poses a significant challenge, resulting in unsatisfactory underwater images.

2.3 Double-Opponency Mechanism

Double-opponency mechanism is a color constancy for color correction proposed by Gao et al [22]. By simulating the characteristics of the retina to the double-opponent cells, the color of the light source in the scene is estimated to be used for the color-biased image. Illuminant $\vec{L} = (L_R, L_G, L_B)$ is calculated by Eq. (1).

$$\begin{pmatrix} L_R \\ L_G \\ L_B \end{pmatrix} = \begin{pmatrix} \max(DOC_R(x)) \\ \max(DOC_G(x)) \\ \max(DOC_B(x)) \end{pmatrix} \quad \textbf{(1)}$$

where max() is the global max pooling, $DOC_R(x)$, $DOC_G(x)$, and $DOC_B(x)$ are the color spaces after the double-opponency cell responds to the RGB image, this response process is shown in Eq. (3). See [22] for specific details. According to the Von Kries model, the color cast image is corrected through Eq. (2).

$$I_c = \vec{L} \times I \tag{2}$$

Where I_c is the corrected image, $\vec{L}$ is the illuminant coefficient, and I is the input image.

$$\begin{pmatrix} DOC_R(x) \\ DOC_G(x) \\ DOC_B(x) \end{pmatrix} = \begin{pmatrix} 1/\sqrt{2} & -1/\sqrt{2} & 0 \\ 1/\sqrt{6} & 1/\sqrt{6} & -2/\sqrt{6} \\ 1/\sqrt{3} & 1/\sqrt{3} & 1/\sqrt{3} \end{pmatrix} \begin{pmatrix} R \\ G \\ B \end{pmatrix} \tag{3}$$

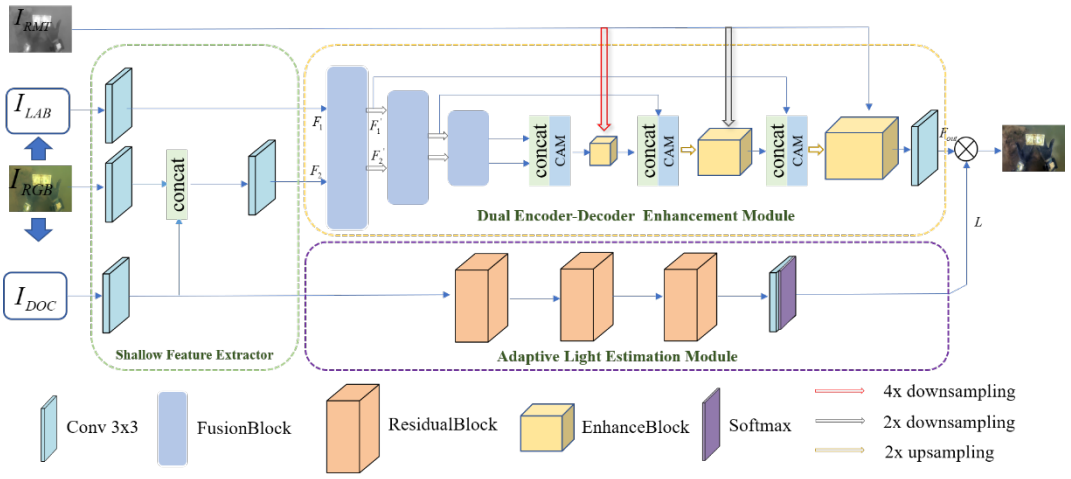

Figure 2. The overall framework of the proposed network

By eliminating the influence of light source, the color distortion of the images can be corrected. Inspired by this theory, we will design a module to extract the corresponding color constancy features for adjusting the tone of the underwater image.

3 Approach

3.1 Proposed Architecture

We propose a model of underwater image enhancement by combining Lab color space and double-opponency mechanism, which is shown in Figure 2. The model has three main modules: shallow feature extractor module, dual encoder-decoder enhancement module, and adaptive light estimation module. Given the input $I = \{I_{RGB}, I_{LAB}, I_{DOC}, I_{RMT}\}$, where I_{RGB} is the underwater degraded image, I_{LAB} is obtained by color space transformation from RGB space, I_{DOC} is the double-opponent space which is converted via Eq. (3), I_{RMT} represents the transmission map of the underwater scene, which can be estimated by the dark channel method [32], shown in Eq. (4).

$$I_{RMT}(x) = \max_{c, x \in \Omega(x)} \left(\frac{B^c - I_{RGB}(x)}{\max(B^c, 1 - B^c)} \right) \tag{4}$$

where B_c is the background light which represents the farthest pixels of I_{RGB}, $\Omega(x)$ denotes a local patch of size 15×15 centered at x, c is the channel of color.

First, we use the shallow feature extractor module to extract features from the RGB, Lab, and double-opponent color space respectively. These features can represent the image information in different color spaces. Next, the extracted features are divided into two branches for processing. The first branch fuses the RGB and Lab information through the encoder part of the dual encoder-decoder enhancement module. I_{RMT} reflects the degree of attenuation degree of light in different range scenes when it propagates in water. The value of I_{RMT} is larger at the close range scene, and less at the distant range, that is the blur degree of distant scenes is more than that of close ones. We use the $1- I_{RMT}$ as a pixel-wise attention map, which is multiplied pixel-wise with the decoded features at the decoder part of the dual encoder-decoder enhancement module. This will enhance the quality of underwater images, especially in distant ranges. The second branch employs the double-opponent space as the input of the adaptive light estimation module, which estimates the light source map corresponding to the underwater image. Finally, the estimated light source map and the output of the decoder part in the first branch are multiplied by element-wise to adjust the overall color of the underwater image deviation. These modules are described in more detail below.

Shallow Feature Extractor. Its role is to obtain features of different color spaces from the input images and convert them into a unified channel dimension. First, we use a 3×3 convolution kernel to conduct convolution processes on the RGB, Lab and double-opponent spaces of input image to obtain feature maps F_{RGB}, F_{LAB} and F_{DOC}. To preserve the information of the double-opponent space on the RGB branch, we concatenate the feature maps F_{DOC} with the F_{RGB} along the channel dimension. After that, we feed F_{DOC} into the adaptive light estimation module to estimate the map of the light source.

Dual Encoder-Decoder Enhancement Module. This module contains encoder and decoder parts. Lab features

and RGB features concatenate with the double-opponent features are used as the input of the encoder part. In the encoder part, we use three fusion blocks, and use 2×2 downsampling between each adjacent fusion block to reduce the spatial resolution of the features. We design a cross fusion residual block as the basic block of each fusion block to fuse Lab and RGB features, as shown in Figure 3. The basic block contains two paths with upper and lower convolution layers, corresponding to the features of RGB and the features of Lab respectively. Each layer accepts feature input, and passes it through a convolution layer. By adding the output features of the other layer, the fused features of the two layers are obtained. Then, two residual features containing the fused information are output from another convolution layer. We use the output of the first fusion block as the input of the second, thereby achieving multiple fusions of the two color space features to improve the representation ability of the features. Eq. (5) and Eq. (6) show the mathematical form of the cross fusion residual block.

$$F_1' = ReLU(W_{12} * (F_{11} + F_{21}) + b_{12}) + F_1 \quad (5)$$

$$F_2' = ReLU(W_{22} * (F_{21} + F_{11}) + b_{22}) + F_2 \quad (6)$$

where F_1 and F_2 are the features of the two input color spaces, and F_{11} are F_{21} the features after the first convolution layer, W and b are the weight and bias terms of the convolution layer respectively.

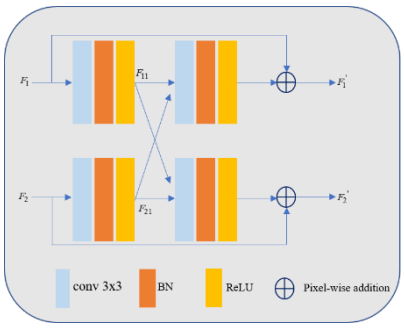

Figure 3. Cross fusion residual block

Before the decoder part, since the extracted features have different attention for the three color spaces that have been fused together. Therefore, the importance of different channels is adaptively adjusted by adding channel attention mechanism [33]. In addition, in order to enhance the details of different distant and near objects in the image, the transmission map of the corresponding scale is introduced in each level enhance block, and the transmission map is used as the spatial attention feature maps to enhance the features by element-wise multiplication. In order to ensure that the transmission map adapts to the different size of the feature maps at different scales in the decoding module, we use max pooling to downsample the transmission map before feeding it into different position of the enhancement module.

Adaptive Light Estimation Module. Images captured underwater are influenced by the absorption of light waves in water, causing image color distortion and a blue-green tint. This phenomenon resembles the imaging under a color-biased light source. Inspired by [22], the double-opponent space is employed to estimate the light source of underwater scenes. An adaptive light estimation module is proposed, which extracts the color constancy by modeling the double-opponent space features, to adjust the overall color of the underwater image. This module consists of three residual blocks, a convolutional layer and a softmax layer, the estimated light source is expressed as:

$$L = Softmax(Conv(Res(Res(Res(F_{DOC}))))) \quad (7)$$

where *Softmax* is the activation layer, *Conv* is 3×3 convolutional layer, *Res* is the residual blocks, F_{DOC} is the features of double-opponent, and L is the estimated light map.

Finally, the features F_{Out} output by the dual encoder-decoder enhancement module and the estimated L are multiplied by elements to obtain an enhanced image, which can be expressed as:

$$output = F_{out} \times L \quad (8)$$

3.2 Network Loss

We use Eq. (9) as the total loss for model training and describe each component of the loss function in detail in the following.

$$\mathcal{L}_{Total} = \mathcal{L}_{L1} + \mathcal{L}_C + \mathcal{L}_{ssim} \quad (9)$$

Pixel-wise Loss (L_{L1}): It usually includes L_{L1} or MSE, which can minimize the gap between the enhanced image I_J' and the clear image I_J. The L_{L1} often generates clearer images than MSE because it is less sensitive to noise and other outliers. In most cases, the L_{L1} is also superior to the MSE loss for reducing color bias from underwater images. Hence, L_{L1} is used as pixel-wise loss and it is shown in Eq. (10).

$$\mathcal{L}_{L1} = \frac{1}{CWH} \sum_{i=1}^{W} \sum_{j=1}^{H} \| I_{J'} - I_J \|_1 \quad (10)$$

VGGLoss (L_C): L_C [34] captures high-level features to ensure the semantic consistency between the enhanced image and the clear image. L_C can avoid over smoothing and enhance the details of the image, as shown in Eq. (11).

$$\mathcal{L}_C = \frac{1}{CWH} \sum_{i=1}^{W} \sum_{j=1}^{H} \| \varphi(I_{J'}) - \varphi(I_J) \|_2 \quad (11)$$

where $\varphi(\cdot)$ is the mid-level features from the 15th convolutional layer of VGG19.

SSIMLoss (L_{ssim}): L_{ssim} is able to effectively evaluate visual quality differences between images. The attenuation, scattering, and chromatic bias of light in water cause underwater images to have blurred details, and color distortion. The aim of L_{ssim} is to optimize the brightness, contrast and structural information of the underwater image. L_{ssim} is shown in Eq. (12).

$$\mathcal{L}_{ssim} = 1 - SSIM \tag{12}$$

SSIM is expressed as:

$$SSIM = \frac{(2\mu_{I_J}\mu_{I_{J'}} + c_1)(\sigma_{I_J I_{J'}} + c_2)}{(\mu_{I_J}^2 + \mu_{I_{J'}}^2 + c_1)(\sigma_{I_J}^2 + \sigma_{I_{J'}}^2 + c_2)} \tag{13}$$

where μ_{I_J} and σ_{I_J} are the mean and standard deviation of the clear image. $\mu_{I_{J'}}$ and $\sigma_{I_{J'}}$ are the mean and standard deviation of the enhanced image. $\sigma_{I_J I_{J'}}$ is the covariance between the enhanced image and the clear image. c_1 and c_2 are constants, generally $c_1 = 0.01^2$ and $c_2 = 0.01^2$.

4 Experiments

4.1 Experimental Details

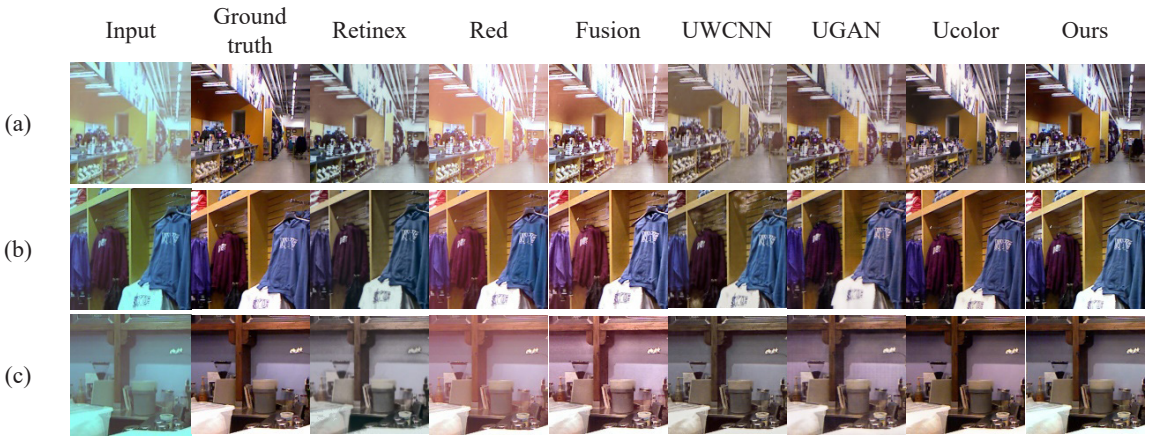

Figure 4. Test results of the proposed method and the six comparison methods on 3 synthetic underwater images (from left to right are: Input, Ground Truth, Retinex [14], Red [13], Fusion [15], UWCNN [23], UGAN [28], Ucolor [30] and Ours)

We jointly train with the UIEB dataset [24] and the synthetic dataset [23]. UIEB comprises 890 real underwater images and corresponding reference images. The synthetic dataset contains 1449 synthetic underwater images of different water bodies. To increase the generalization of the proposed model, we mix 800 pairs of real underwater images and 1350 pairs of synthetic underwater images from these two datasets as the training data. Meanwhile, we randomly select 90 pairs of real underwater images and reference images from the UIEB dataset and 30 pairs of synthetic underwater images from the synthetic dataset as the test data. Table 1 shows the configuration of all the experiments.

Table 1. Experimental setup

Framework	Pytorch
Optimizer	Adam
Total epoch	500
Batch size	16
Learning rate	0.0002
GPU	V100 (32G)

4.2 Qualitative Evaluations and Quantitative Evaluations

We evaluate the performance of six other methods: Retinex [14], Red [13], Fusion [15], UWCNN [23], UGAN [28], and Ucolor [30]. We select different scenes from the synthetic dataset as test samples, and Figure 4 shows the results on synthetic underwater images. The Red and Fusion methods eliminate the green color, but introduce severe red distortion, while Retinex performs better in color restoration than the previous two methods, but fails to preserve the image sharpness. These three traditional methods are obviously not adapted to the synthetic dataset, and thus produce unsatisfactory results. UWCNN effectively removes the underwater artifacts, but it also alters some of the original colors of the images, resulting in a slight deviation from the ground truth, whereas UGAN performs poorly in image clarity. Ucolor tends to produce warmer colors in recovering the underwater images (e.g. (c) in Figure 4). Ours surpasses the others in both color and sharpness aspects. Three traditional methods achieve low scores on PSNR/SSIM in Table 2, which agrees with the visual results. Among the deep learning methods, our proposed method significantly surpasses UWCNN and UGAN, and also outperforms Ucolor by a large margin on PSNR. Based on this analysis, our proposed method excels at enhancing underwater images compared to the other methods.

Moreover, we test on UIEB, as shown in Figure 5. In scene (a), the Red, UWCNN, and Ucolor methods all produce slightly blurred images, while the Retinex method introduces obvious artifacts. In scene (b), the Red and

produce slightly blurred images, while the Retinex method introduces obvious artifacts. In scene (b), the Red and Fusion methods cause a slight green shift to the coral reefs in the background, while the proposed method removes the underwater effect and restores more realistic colors. In scenes (c) and (d), the contrastive methods lack texture details, have artifacts, and suffer from green shifts (e.g. Red and Ucolor). Based on visual effects, our approach significantly improves the color and clarity of underwater images, verifying the effectiveness of fusing Lab and double-opponent in this paper.

Table 2. PSNR/SSIM scores of six methods and the proposed method on the synthetic dataset

Method	PSNR↑	SSIM↑
Retinex	16.54	0.81
Red	13.72	0.78
Fusion	15.81	0.82
UWCNN	19.24	0.88
UGAN	19.72	0.86
Ucolor	23.49	0.94
Ours	**25.67**	**0.95**

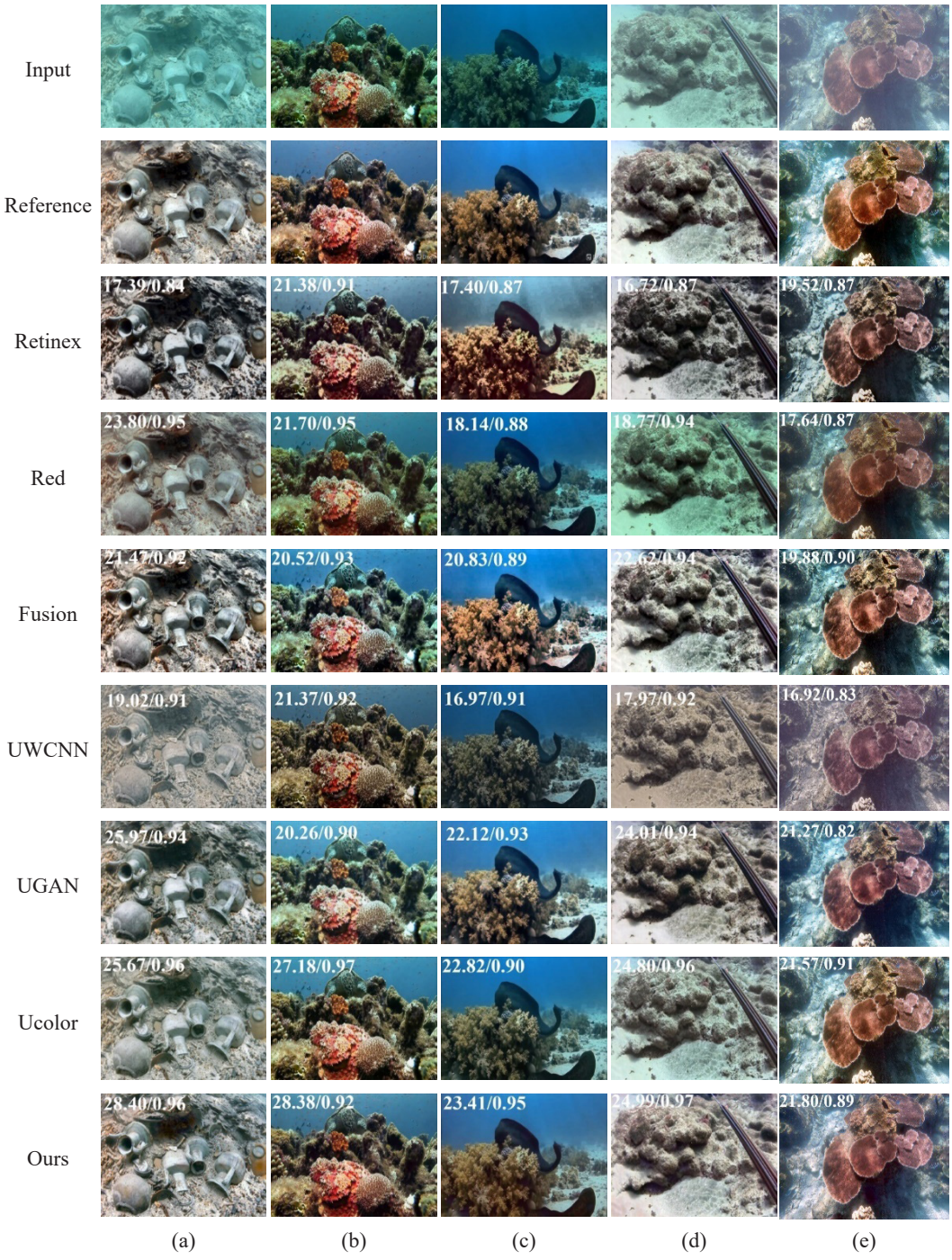

Figure 5. The proposed method and other comparison methods are tested on the UIEB dataset (from top to bottom are: input, Reference, Retinex, Red, Fusion, Ucolor and Ours. The numbers in the upper left corner of the image indicate PSNR/SSIM)

In addition to visual effect analysis, we evaluate the enhancement effect using reference metrics (PSNR/SSIM) and non-reference metrics (UIQM [35]/UCIQE [36]). The reference image is used as the ground-truth for calculating the reference metrics. Table 3 shows the results on the PSNR and SSIM, where higher scores indicate better results. Our model significantly outperforms the comparison methods on the PSNR, and is only slightly behind the Ucolor method on the SSIM, with a gap of only 0.01. For the non-reference metrics, we use UIQM/UCIQE to measure the enhancement effect. UIQM is more similar with the human eye perception, and higher scores indicate better results. UCIQE focuses on the color distortion, color saturation and other color-related features of the image, and higher scores indicate better results. Table 4 presents the performance scores of our model and the comparison methods on UIQM/UCIQE. As observed in the table, our model surpasses the comparison methods on both non-reference metrics. By combining the visual effect and objective metrics, we demonstrate that Ours significantly improves underwater image enhancement.

Table 3. PSNR/SSIM scores of six methods and the proposed method on the real underwater images

Method	PSNR ↑	SSIM ↑
Retinex	18.31	0.84
Red	19.10	0.86
Fusion	20.55	0.89
UWCNN	18.81	0.84
UGAN	21.38	0.89
Ucolor	21.27	**0.92**
Ours	**21.65**	0.91

Table 4. UIQM/UCIQE scores of six methods and the proposed on the real underwater images

Method	UIQM ↑	UCIQE ↑
Retinex	2.75	1.87
Red	2.54	1.55
Fusion	2.72	1.78
UWCNN	2.71	1.53
UGAN	2.81	1.33
Ucolor	2.79	1.47
Ours	**2.97**	**1.94**

4.3 Ablation Study

We conduct ablation experiments to verify the functions of VGGLoss and SSIMLos. Figure 6 illustrates the visual results. w/o L_C & L_{ssim} denotes the case without VGGLoss and SSIMLoss. w/o L_{ssim} denotes the case without SSIMLoss. Comparing the two groups of plots w/o L_C & L_{ssim} and w/o L_{ssim}, w/o L_C & L_{ssim} causes the images to be artifactual and unrealistic. w/o L_{ssim} will decrease the contrast and colorfulness of the underwater images. We also perform a quantitative analysis of the experimental results of Figure 6 using the PSNR/SSIM scores in Table 5. It indicates that adding VGGLoss can improve the PSNR/SSIM scores. When VGGLoss is used in combination with SSIMLoss, the PSNR/SSIM scores are further improved.

In addition, we conduct ablation experiments by removing I_{RMT}, I_{LAB} and I_{DOC} inputs respectively to analyze effectiveness. As shown in Figure 7 and Table 5, after removing the I_{RMT}, the enhancement effect in some areas (red box of Figure 7) of the image is noticeably blured, and exhibits color distortion and low contrast. This further verifies that I_{RMT} can contribute to improve the model

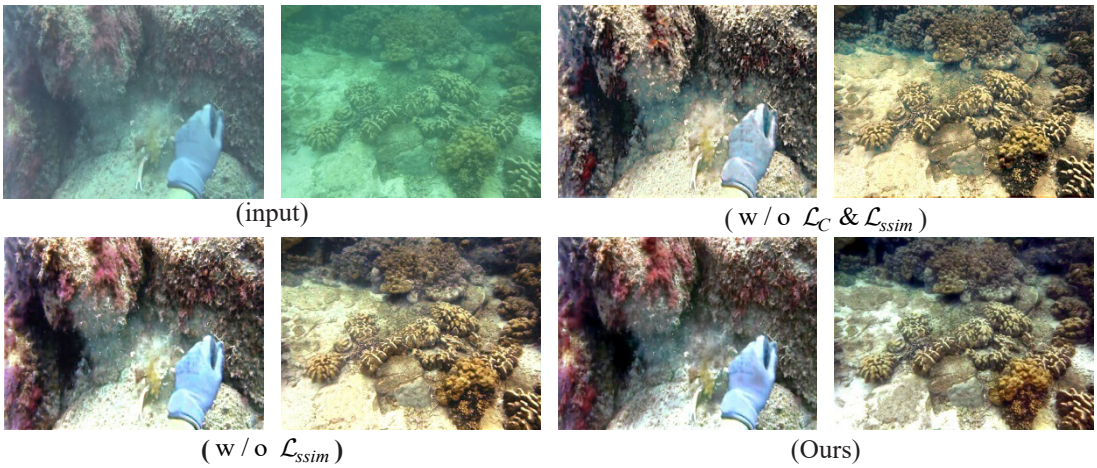

Figure 6. Ablation study towards the $\mathcal{L}_C$ and the $\mathcal{L}_{ssim}$

Figure 7. Ablation study towards the I_{RMT}, I_{LAB} and I_{DOC}

performance by assigning depth weights to the degradation regions.On the other hand, the results of without I_{DOC} are partially overexposed and color distorted, which indicates that I_{DOC} can effectively balance the brightness and saturation of the image. Similarly, removing I_{LAB} leads to over-enhanced color the artificial edge. In contrast, our proposed method achieves superior visual results, effectively suppressing noise while better preserving color restoration and detail enhancement.

Table 5. Quantitative results of the ablation study in terms of average PSNR and SSIM values

Method	PSNR↑	SSIM↑
w / o $\mathcal{L}_C$ & $\mathcal{L}_{ssim}$	18.13	0.84
w / o $\mathcal{L}_{ssim}$	18.68	0.88
w / o I_{LAB}	17.04	0.79
w / o $\mathcal{L}_{DOC}$	17.11	0.86
w / o I_{RMT}	19.28	0.87
Ours	**21.65**	**0.91**

5 Conclusion and Discussion

In this paper, we have integrated human visual perception and color constancy mechanism into the field of image enhancement, and propose an underwater image enhancement model that combines Lab color space and double-opponent mechanism. Lab color space has a wider range of tones than RGB. By integrating the color information of Lab and RGB, a dual encoder-encoder enhancement module is designed, which can extract richer hue information and improve local details of the input image. For the first time, the double-opponent mechanism, which can resist the change of light source in different environments, is applied to the deep learning model. By leveraging the double-opponent features, an adaptive light estimation module is designed to extract the light source map to compensate for the color deviation of underwater images.

The experiment results verify that our approach can correct the color deviation in complex environments, and achieve better visibility and natural appearance. Moreover, it also improves the clarity of the underwater images. The quantitative comparisons have indicated that image quality assessment indicators have been improved compared with those of the other enhancement approaches.

We also found that the performance of the proposed model is still a certain gap between the real underwater image and the synthetic image, especially in the waters with high turbidity. This may be due to environmental differences between the synthetic images involved in the training and the real underwater images. As the labels of real underwater images are difficult to obtain, we will consider generating more realistic environment simulation data in water or effective semi-supervised learning methods to improve the generalization and robustness of the underwater enhancement model in the future.

Acknowledgement

This research was supported by the Yantai Science and Technology Innovation Development Plan Basic Research Project (Grant No. 2023JCYJ044). The authors also gratefully acknowledge the reviewers' helpful comments and suggestions, which will improve the presentation significantly.

References

[1] D. Akkaynak, T. Treibitz, T. Shlesinger, Y. Loya, R. Tamir, D. Iluz, What is the space of attenuation coefficients in underwater computer vision? *Proceedings of the IEEE Conference on Computer Vision and Pattern Recognition (CVPR)*, Honolulu, HI, USA, 2017, pp. 568-577. https://doi.org/10.1109/CVPR.2017.68

[2] J.-Y. Chiang, Y.-C. Chen, Underwater image enhancement by wavelength compensation and dehazing, *IEEE Transactions on Image Processing*, Vol. 21, No. 4, pp. 1756-1769, April, 2012. https://doi.org/10.1109/TIP.2011.2179666

[3] P. Zhuang, J. Wu, F. Porikli, C. Li, Underwater image enhancement with hyper-laplacian reflectance Priors, *IEEE Transactions on Image Processing*, Vol. 31, pp. 5442-5455,

August, 2022.
https://doi.org/10.1109/TIP.2022.3196546

[4] D. Akkaynak, T. Treibitz, A revised underwater image formation model, *Proceedings of the IEEE Conference on Computer Vision and Pattern Recognition (CVPR)*, Salt Lake City, UT, USA, 2018, pp. 6723-6732.
https://doi.org/10.1109/CVPR.2018.00703

[5] J. Zhou, T. Yang, W. Chu, W. Zhang, Underwater image restoration via backscatter pixel prior and color compensation, *Engineering Applications of Artificial Intelligence*, Vol. 111, Article No. 104785, May, 2022.
https://doi.org/10.1016/j.engappai.2022.104785

[6] J. Zhou, J. Sun, W. Zhang, Z. Lin, Multi-view underwater image enhancement method via embedded fusion mechanism, *Engineering Applications of Artificial Intelligence*, Vol. 121, Article No. 105946, May, 2023.
https://doi.org/10.1016/j.engappai.2023.105946

[7] Q. Qi, Y. Zhang, F. Tian, Q. J. Wu, K. Li, X. Luan, D. Song, Underwater image co-enhancement with correlation feature matching and joint learning, *IEEE Transactions on Circuits and Systems for Video Technology*, Vol. 32, No. 3, pp. 1133–1147, March, 2022.
https://doi.org/10.1109/TCSVT.2021.3074197

[8] D. Akkaynak, T. Treibitz, Sea-Thru: A method for removing water from underwater images, *Proceedings of the IEEE/CVF Conference on Computer Vision and Pattern Recognition (CVPR)*, Long Beach, CA, USA, 2019, pp. 1682-1691.
https://doi.org/10.1109/CVPR.2019.00178

[9] B. Yao, X. Cao, B. Shen, G. Li, J. Yin, Location of Static Targets on the Seabed: A Study, *Journal of Internet Technology*, Vol. 21, No. 5, pp. 1563-1569, September, 2020.
https://doi.org/10.3966/160792642020092105028

[10] M. Jian, H. Yu, Towards reliable object representation via sparse directional patches and spatial center cues, *Fundamental Research*, Vol. 5, No. 1, pp. 354-359, January, 2025.
https://doi.org/10.1016/j.fmre.2023.08.001

[11] J. S. Jaffe, Computer modeling and the design of optimal underwater imaging systems, *IEEE Journal of Oceanic Engineering*, Vol. 15, No. 2, pp. 101-111, April, 1990.
https://doi.org/10.1109/48.50695

[12] P. L. J. Drews, E. R. Nascimento, S. S. C. Botelho, M. F. M. Campos, Underwater depth estimation and image restoration based on single images, *IEEE Computer Graphics and Applications*, Vol. 36, No. 2, pp. 24-35, March-April, 2016.
https://doi.org/10.1109/MCG.2016.26

[13] A. Galdran, D. Pardo, A. Picon, A. Alvarez-Gila, Automatic red-channel underwater image restoration, *Journal of Visual Communication and Image Representation*, Vol. 26, pp. 132–145, January, 2015.
https://doi.org/10.1016/j.jvcir.2014.11.006

[14] X. Fu, P. Zhuang, Y. Huang, Y. Liao, X.-P. Zhang, X. Ding, A retinex-based enhancing approach for single underwater image, *2014 IEEE International Conference on Image Processing (ICIP)*, Paris, France, 2014, pp. 4572-4576.
https://doi.org/10.1109/ICIP.2014.7025927

[15] C. Ancuti, C. O. Ancuti, T. Haber, P. Bekaert, Enhancing underwater images and videos by fusion, *Proceedings of the IEEE Conference on Computer Vision and Pattern Recognition (CVPR)*, Providence, RI, USA, 2012, pp. 81-88.
https://doi.org/10.1109/CVPR.2012.6247661

[16] N. Wang, H. Zheng, B. Zheng, Underwater image restoration via maximum attenuation identification, *IEEE Access*, Vol. 5, pp. 18941-18952, September, 2017.
https://doi.org/10.1109/ACCESS.2017.2753796

[17] Y.-T. Peng, P. C. Cosman, Underwater image restoration based on image blurriness and light absorption, *IEEE Transactions on Image Processing*, Vol. 26, No. 4, pp. 1579-1594, April, 2017.
https://doi.org/10.1109/TIP.2017.2663846

[18] J.-Y. Zhu, T. Park, P. Isola, A. A. Efros, Unpaired image-to-image translation using cycle-consistent adversarial networks, *Proceedings of the IEEE International Conference on Computer Vision (ICCV)*, Venice, Italy, 2017, pp. 2242-2251.
https://doi.org/10.1109/ICCV.2017.244

[19] Z. Fu, W. Wang, Y. Huang, X. Ding, K.-K. Ma, Uncertainty inspired underwater image enhancement, *European Conference on Computer Vision (ECCV)*, Tel Aviv, Israel, 2022, pp. 465-482.
https://doi.org/10.1007/978-3-031-19797-0_27

[20] X. Fu, Z. Fan, M. Ling, Y. Huang, X. Ding, Two-step approach for single underwater image enhancement, *2017 International Symposium on Intelligent Signal Processing and Communication Systems (ISPACS)*, Xiamen, China, 2017, pp. 789-794.
https://doi.org/10.1109/ISPACS.2017.8266583

[21] H. Zhou, B. Yao, K. Ye, G. Li, J. Guo, Research on underwater noise features based on spectrum analysis and Welch algorithm, *Journal of Internet Technology*, Vol. 22, No. 3, pp. 715-723, May, 2021.
https://doi.org/10.3966/160792642021052203020

[22] S.-B. Gao, K.-F. Yang, C.-Y. Li, Y.-J. Li, Color constancy using double-opponency, *IEEE Transactions on Pattern Analysis and Machine Intelligence*, Vol. 37, No. 10, pp. 1973-1985, October, 2015.
https://doi.org/10.1109/tpami.2015.2396053

[23] C. Li, S. Anwar, F. Porikli, Underwater scene prior inspired deep underwater image and video enhancement, *Pattern Recognition*, Vol. 98, Article No. 107038, February, 2020.
https://doi.org/10.1016/j.patcog.2019.107038

[24] C. Li, C. Guo, W. Ren, R. Cong, J. Hou, S. Kwong, D. Tao, An underwater image enhancement benchmark dataset and beyond, *IEEE Transactions on Image Processing*, Vol. 29, pp. 4376-4389, November, 2019.
https://doi.org/10.1109/TIP.2019.2955241

[25] M. S. Hitam, E. A. Awalludin, W. N. J. H. W. Yussof, Z. Bachok, Mixture contrast limited adaptive histogram equalization for underwater image enhancement, *2013 International Conference on Computer Applications Technology (ICCAT)*, Sousse, Tunisia, 2013, pp. 1-5.
https://doi.org/10.1109/ICCAT.2013.6522017

[26] C.-Y. Li, J.-C. Guo, R.-M. Cong, Y.-W. Pang, B. Wang, Underwater image enhancement by dehazing with minimum information loss and histogram distribution prior, *IEEE Transactions on Image Processing*, Vol. 25, No. 12, pp. 5664-5677, December, 2016.
https://doi.org/10.1109/TIP.2016.2612882

[27] J. Li, K. A. Skinner, R. M. Eustice, M. Johnson-Roberson, WaterGAN: unsupervised generative network to enable real-time color correction of monocular underwater images, *IEEE Robotics and Automation Letters*, Vol. 3, No. 1, pp. 387-394, January, 2018. https://doi.org/10.1109/LRA.2017.2730363

[28] C. Fabbri, M. J. Islam, J. Sattar, Enhancing underwater imagery using generative adversarial networks, *2018 IEEE*

International Conference on Robotics and Automation (ICRA), Brisbane, QLD, Australia, 2018, pp. 7159-7165. https://doi.org/10.1109/ICRA.2018.8460552

[29] L. Peng, C. Zhu, L. Bian, U-shape transformer for underwater image enhancement, *IEEE Transactions on Image Processing*, Vol. 32, pp. 3066-3079, May, 2023. https://doi.org/10.1109/TIP.2023.3276332

[30] C. Li, S. Anwar, J. Hou, R. Cong, C. Guo, W. Ren, Underwater image enhancement via medium transmission-guided multi-color space embedding, *IEEE Transactions on Image Processing*, Vol. 30, pp. 4985-5000, May, 2021. https://doi.org/10.1109/TIP.2021.3076367

[31] Z. Zhang, H. Yan, K. Tang, Y. Duan, *MetaUE: model-based meta-learning for underwater image enhancement*, March, 2023. https://arxiv.org/abs/2303.06543

[32] K. He, J. Sun, X. Tang, Single image haze removal using dark channel prior, *IEEE Transactions on Pattern Analysis and Machine Intelligence*, Vol. 33, No. 12, pp. 2341–2353, December, 2011. https://doi.org/10.1109/TPAMI.2010.168

[33] J. Hu, L. Shen, S. Albanie, G. Sun, E. Wu, Squeeze-and-excitation networks, *IEEE Transactions on Pattern Analysis and Machine Intelligence*, Vol. 42, No. 8, pp. 2011-2023, August, 2020. https://doi.org/10.1109/TPAMI.2019.2913372

[34] C. Ledig, L. Theis, F. Huszár, J. Caballero, A. Cunningham, A. Acosta, A. Aitken, A. Tejani, J. Totz, Z. Wang, W. Shi, Photo-realistic single image super-resolution using a generative adversarial network, *Proceedings of the IEEE Conference on Computer Vision and Pattern Recognition (CVPR)*, Honolulu, HI, USA, 2017, pp. 105-114. https://doi.org/10.1109/CVPR.2017.19

[35] M. Yang, A. Sowmya, An underwater color image quality evaluation metric, *IEEE Transactions on Image Processing*, Vol. 24, No. 12, pp. 6062-6071, December, 2015. https://doi.org/10.1109/TIP.2015.2491020

[36] K. Panetta, C. Gao, S. Agaian, Human-visual-system-inspired underwater image quality measures, *IEEE Journal of Oceanic Engineering*, Vol. 41, No. 3, pp. 541-551, July, 2016. https://doi.org/10.1109/JOE.2015.2469915

Biographies

Xing Huang received the B.S. degree in the School of Electronics and Information Engineering from Jinggangshan University in 2020, and now he is studying for a master's degree in computer science and technology in Ludong University. His current research interests include underwater image enhancement, image restoration, super-resolution, etc.

Yujuan Sun received the Ph.D. degree from the Department of Computer Science and Technology, Ocean University of China. She joined the College of Information and Electrical Engineering at Ludong University as an associate professor. She has published about 30 papers in international journals and conferences, and her research interests include underwater image enhancement, 3D reconstruction, pattern recognition, etc.

Xiaofeng Zhang received the B.S. degree and the Master Degree from the School of Computer and Communication, Lanzhou University of Technology, Lanzhou, China, in 2000 and 2005, respectively. He received the Ph.D. Degree from the School of Computer Science and technology of Shandong University in 2014. Now he is a professor with the School of Information and Electrical Engineering of Ludong University, and with Shandong Provincial Key Laboratory of Digital Media Technology. His research interests include image segmentation, machine learning, etc.

Jiaxing Zhang received the B.S. degree in the School of Information Engineering from Nanchang University in 2019, and now she is studying for a master's degree in computer science and technology in Ludong University. Her research focuses on image segmentation.